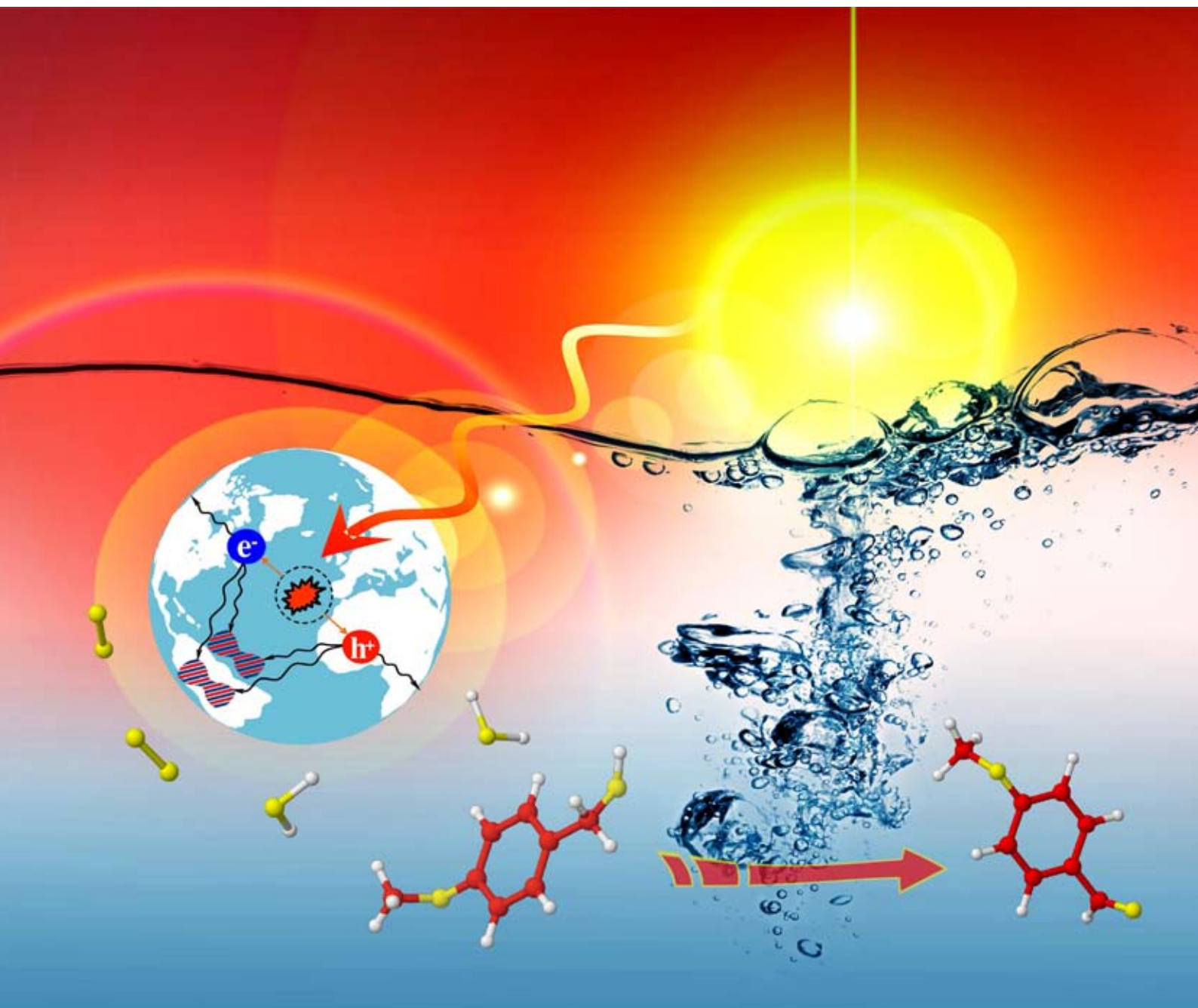


# Green Chemistry

Cutting-edge research for a greener sustainable future

[www.rsc.org/greenchem](http://www.rsc.org/greenchem)

Volume 11 | Number 4 | April 2009 | Pages 437–592



ISSN 1463-9262

Ravasio *et al.*  
Selective hydrogenation of oils

Palmisano *et al.*  
Photocatalytic oxidation of aromatic  
alcohols in water

Clark *et al.*  
Microwave-assisted preparation of amides

Pol *et al.*  
Solvent free process for the generation  
of conducting carbon spheres



1463-9262(2009)11:4;1-A

RSC Publishing

# Selective photocatalytic oxidation of 4-substituted aromatic alcohols in water with rutile TiO<sub>2</sub> prepared at room temperature†

Sedat Yurdakal,<sup>a,b</sup> Giovanni Palmisano,<sup>a</sup> Vittorio Loddo,<sup>a</sup> Oğuzhan Alagöz,<sup>c</sup> Vincenzo Augugliaro<sup>\*a</sup> and Leonardo Palmisano<sup>\*a</sup>

Received 7th November 2008, Accepted 27th January 2009

First published as an Advance Article on the web 18th February 2009

DOI: 10.1039/b819862d

Home-prepared (HP) rutile TiO<sub>2</sub> catalysts were prepared at room temperature by using H<sub>2</sub>O and TiCl<sub>4</sub> in different ratios and without addition of additives. The catalysts were used for carrying out the selective photocatalytic oxidation of 4-methoxybenzyl alcohol to 4-methoxybenzaldehyde in aqueous suspension, free from any organic co-solvent. The selectivities showed by the home prepared catalysts were in the 45–74% range, up to four times higher than that of a commercial rutile TiO<sub>2</sub> sample, the reaction rates being comparable. By using the most selective photocatalyst, the oxidation of benzyl, 4-methylbenzyl, and 4-nitrobenzyl alcohols was also carried out in order to investigate the influence of the substituent group on the oxidation rate and selectivity. The presence of an –OCH<sub>3</sub> group positively influenced the selectivity whereas a –NO<sub>2</sub> group showed to have a detrimental effect. The Hammett relationship effectively describes the influence of substituent group on the kinetic constant of partial oxidation of aromatic alcohols to aldehydes.

## 1. Introduction

Among the advanced oxidation processes investigated in the last decades, photocatalysis in the presence of an irradiated semiconductor has proven to be very effective in the field of environment remediation. The use of irradiation to initiate chemical reactions is the principle on which heterogeneous photocatalysis is based; in fact, when a semiconductor oxide is irradiated with suitable light, excited electron–hole pairs result that can be applied in chemical processes to modify specific compounds. The main advantage of heterogeneous photocatalysis, when compared with the chemical methods, is that in most cases it is possible to obtain a complete mineralization of the toxic substrate even in the absence of added reagents. The radical mechanism of photocatalytic reactions, which involve fast attacks of strongly oxidant hydroxyl radicals,<sup>1</sup> determines their unselective features. Additional advantages are: (i) its non-specificity; (ii) the possibility of treating effluents having very low concentrations of contaminants without lowering the reaction rate to negligible values; (iii) the possibility of operation at ambient temperature and pressure; (iv) the use of a cheap oxidant, *i.e.* molecular oxygen.

Various semiconductor materials have been tested as oxidation photocatalysts, but it is generally accepted that anatase TiO<sub>2</sub> is the most reliable material due to its low cost, high photostability and its ability to be activated by near UV-light and also by the solar radiation. Among the crystalline phases of TiO<sub>2</sub> (anatase, rutile and brookite), anatase, pure or in mixture with rutile, shows the highest activity. Rutile, which is the most thermodynamically stable phase, usually shows scarce photo-activity. Likely reasons invoked to explain the poor performance of rutile with respect to anatase phase are that it shows a very low hydroxyl group surface concentration and a high recombination rate of the photogenerated e<sup>–</sup>–h<sup>+</sup> pairs.<sup>2–5</sup> However, while rutile produced at very high temperature (*ca.* 1000 K) shows a poor photoreactivity,<sup>6</sup> rutile home prepared at low temperature exhibits a certain photocatalytic activity.<sup>7</sup> The preparation of photo-active rutile samples is generally carried out at room temperature in highly concentrated acidic solutions. Yin *et al.*,<sup>8</sup> for instance, crystallized TiO<sub>2</sub> at room temperature in the presence of HCl, HNO<sub>3</sub> or H<sub>2</sub>SO<sub>4</sub> by using titanium tetraisopropoxide as the precursor. It is worth noting that in the absence of acids they obtained amorphous TiO<sub>2</sub>. Yang *et al.*<sup>9</sup> used Ti(SO<sub>4</sub>)<sub>2</sub> as the precursor but the crystallization occurred after a long time and in HNO<sub>3</sub> solution. Fei *et al.*<sup>10</sup> prepared rutile nanorods photo-active for the degradation of harmful molecules, starting from titanium isopropoxide solution at room temperature in a concentrated HNO<sub>3</sub> solution.

The partial oxidation of –CH<sub>2</sub>OH to –CHO group is a key reaction step throughout many organic syntheses; this reaction is commonly used in the preparation of many organic products, due to the wide use of aldehyde derivatives in the flavour, confectionary, and beverage industries.<sup>11</sup> Generally the conditions, in which the industrial synthetic processes are carried out, are environmentally harmful as they involve organic solvents at high temperature and pressure and stoichiometric oxygen donors that

<sup>a</sup>“Schiavello-Grillone” Photocatalysis Group – Dipartimento di Ingegneria Chimica dei Processi e dei Materiali, Università degli Studi di Palermo, Viale delle Scienze, 90128, Palermo, Italy. E-mail: augugliaro@dicpm.unipa.it, palmisano@dicpm.unipa.it; Fax: +39 091 23863768; Tel: +39 091 23863746

<sup>b</sup>Kimya Bölümü, Fen Fakültesi, Anadolu Üniversitesi, Yunus Emre Kampüsü, 26470, Eskişehir, Turkey

<sup>c</sup>Kimya Bölümü, Fen Fakültesi, Ankara Üniversitesi, Tandoğan, 06100, Ankara, Turkey

† Electronic supplementary information (ESI) available: SEM images and NMR analysis. See DOI: 10.1039/b819862d

are not only expensive and toxic compounds but also produce high amounts of dangerous wastes.

Selective photocatalysed oxidation of diols to the corresponding hydroxy-carbonylic compounds was carried out in aqueous acetonitrile<sup>12</sup> or dichloromethane<sup>13</sup> TiO<sub>2</sub> suspensions; decatungstate anion<sup>14</sup> heterogenized on silica was also used in dichloromethane solvent. It was found that the adsorption of the diol is an important parameter able to affect efficiency and selectivity of the photocatalytic process. Photocatalytic oxidation of aromatic alcohol has been carried out either in acetonitrile medium<sup>15</sup> or in air.<sup>16</sup> However, recently partial oxidation of aromatic alcohol has been carried out in water suspensions. 4-Methoxybenzyl alcohol (MBA) has been partially oxidized to 4-methoxybenzaldehyde (MBAD): a 10% selectivity was found by using Degussa P25 whereas by using HP anatase-rutile samples obtained with different aging times<sup>17</sup> at 373 K a higher selectivity was obtained (up to 41% with pure anatase). By using a similar preparation method pure brookite sample<sup>18</sup> showed higher selectivity than pure rutile (39% and 32%, respectively). Later on, 60% of selectivity was attained with home prepared rutile synthesised at 333 K under similar experimental conditions.<sup>19</sup> The investigation of the reaction pathway<sup>17-19</sup> indicated that in all cases the MBA photocatalytic oxidation proceeds through two parallel reaction routes: the first one determines the MBA partial oxidation to MBAD while the second one eventually causes the direct mineralization of MBA to CO<sub>2</sub>. This last pathway occurs through a series of reactions taking place over the catalyst surface and producing intermediates not desorbing to the bulk of solution. It was found that the increase of aging time increases both the rutile/anatase ratio, the crystallinity of catalysts and the activity for alcohol oxidation but it decreases the selectivity to aldehyde. In the competition between partial and complete oxidation, more crystalline catalysts favour the complete oxidation while less crystalline or amorphous catalysts, even if less reactive, favour the partial oxidation. The influence of calcination temperature on catalyst crystallinity, photoreactivity and selectivity was also investigated by using pure rutile samples. The crystallinity always increased while the reactivity showed a maximum at 673 K and then it decreased owing to the surface dehydroxylation. As expected the selectivity continuously decreased, the highest one being obtained with lesser crystalline sample. In order to find likely explanations for the different photo-activity shown by home prepared anatase and commercial catalysts, their textural, bulk and surface properties have been investigated.<sup>20,21</sup> It was found that the textural and intrinsic electronic features of catalysts were almost the same; on the contrary ATR-FTIR studies indicated that the higher selectivity found for home-made catalysts with respect to commercial ones is related to their low crystallinity and to their high surface hydroxyl group density that induces an enhanced hydrophilicity of the TiO<sub>2</sub> surface. Both of these properties promote the desorption of the photo-produced aldehyde thus hindering its further oxidation.

In the present work, TiO<sub>2</sub> rutile catalysts have been obtained at room temperature with a preparation method in milder conditions than those previously reported. These catalysts have been used to investigate the selective photo-oxidation of MBA to MBAD in water. In order to investigate if the reaction selectivity towards the partial oxidation depends on the catalyst

**Table 1** 4-substituted alcohols and corresponding aldehydes

-R	Alcohol	Aldehyde
-H	BA	BAD
-OCH <sub>3</sub>	MBA	MBAD
-CH <sub>3</sub>	MeBA	MeBAD
-NO <sub>2</sub>	NBA	NBAD

or also on the chemical nature of aromatic alcohol used, the photocatalytic oxidation of some 4-substituted benzyl alcohols to the corresponding aldehydes (see Table 1), *i.e.* benzyl alcohol (BA) to benzaldehyde (BAD), 4-methylbenzyl alcohol (MeBA) to 4-methylbenzaldehyde (MeBAD) and 4-nitrobenzyl alcohol (NBA) to 4-nitrobenzaldehyde (NBAD), has been investigated by using the same HP rutile sample. For the sake of comparison a commercial rutile TiO<sub>2</sub> (Sigma Aldrich, SA) sample was also tested under the same experimental conditions used for all the HP samples.

## 2. Experimental

### 2.1 Catalyst Preparation and characterization

The precursor solutions were obtained by adding 20 mL of TiCl<sub>4</sub> (> 97%, Fluka) to 400, 700, 1000, 1500 or 2000 mL water contained in a volumetric flask; the addition was carried out very slowly without agitation in order to avoid the warming of the solution as the TiCl<sub>4</sub> hydrolysis is a highly exothermic reaction. At the end of the addition, the resulting solution was mixed for 2 min by a magnetic stirrer and then the flask was sealed and maintained at room temperature (*ca.* 298 K) for a total aging time ranging from 4 to 9 days. Just after *ca.* 12 h aging, the sol became a transparent solution and then, after waiting a few days, the precipitation process started. The solid powder that precipitated at the end of the whole treatment was separated by centrifugation (20 min at 5000 rpm) and dried at room temperature. The final home-prepared (HP) catalysts are hereafter indicated as HP1/20, HP1/35, HP1/50, HP1/75 and HP1/100 where the numbers indicate the TiCl<sub>4</sub>/H<sub>2</sub>O volumetric ratio.

XRD patterns of the powders were recorded by a Philips diffractometer using the Cu K $\alpha$  radiation and a 2 $\theta$  scan rate of 1.28° min<sup>-1</sup>. SEM images were obtained using an ESEM microscope (Philips, XL30) operating at 25 kV. A thin layer of gold was evaporated on catalysts samples, previously sprayed on the stab and dried at room temperature. BET specific surface areas were measured by the single-point BET method using a Micromeritics Flow Sorb 2300 apparatus.

Before the analysis, the samples were dried for 1 h at 100 °C, for 2 h at 150 °C and degassed for 0.5 h at 150 °C.

### 2.2 Photoreactivity set up and procedure

A cylindrical Pyrex batch photoreactor with an immersed lamp, containing 0.5 L of aqueous suspension, was used to perform the reactivity experiments. The photoreactor was provided with ports in its upper section for the inlet and outlet of oxygen and for sampling. A magnetic stirrer guaranteed a satisfactory

suspension of the photocatalyst and the homogeneity of the reacting mixture. A 125 W medium pressure Hg lamp (Helios Italquartz, Italy), axially positioned within the photoreactor, was cooled by water circulating through a Pyrex thimble; the temperature of the suspension was about 300 K. The radiation energy impinging on the suspension had an average value of 10 mW cm<sup>-2</sup>. It was measured at 360 nm by using a radiometer UVX Digital.

The initial concentration used for MBA, BA, MeBA and NBA was 1 mM. Since the surface area and the agglomerate size of the various photocatalysts were different, the photoreactivity runs were carried out at equal irradiation conditions of the suspension, *i.e.* at equal flow of photons absorbed by the suspensions. For each catalyst the amount chosen for the photocatalytic runs was that for which the resulting suspension was able to absorb 90% of the impinging radiation. This choice also guaranteed that all the catalyst particles were irradiated. Measurements of the transmitted light in the presence of the suspension were carried out by using the radiometer above described. An amount of 0.2 g L<sup>-1</sup> was used for HP1/20, HP1/75 and HP1/100 samples, 0.4 g L<sup>-1</sup> for the commercial SA catalyst, while an amount of 0.6 g L<sup>-1</sup> was required for HP1/35 and HP1/50 samples. A selected run of MBA photo-oxidation was carried out by using 0.2 g L<sup>-1</sup> of HP1/50. NaOH 1 M solution was used to adjust the initial pH to 7.

Before switching on the lamp, oxygen was bubbled into the suspension for 30 min at room temperature to reach the thermodynamic equilibrium. Adsorption of the alcohols under dark conditions was always quite low, *i.e.* less than 5%. During the run, samples of reacting suspension were withdrawn at fixed time intervals; they were immediately filtered through a 0.45 μm hydrophilic membrane (HA, Millipore) before being analysed.

The quantitative determination and identification of the species present in the reacting suspension was performed by means of a Beckman Coulter HPLC (System Gold 126 Solvent Module and 168 Diode Array Detector), equipped with a Luna 5 μ Phenyl-Hexyl column (250 mm long × 2 mm id), using Sigma Aldrich standards. Retention times and UV spectra of the compounds were compared with those of standards. The eluent consisted of: 17.5% acetonitrile, 17.5% methanol, 65% 40 mM KH<sub>2</sub>PO<sub>4</sub> aqueous solution. TOC analyses were carried out by using a 5000 A Shimadzu TOC analyser. All the used chemicals were purchased from Sigma Aldrich with a purity > 99.0%.

A specific photocatalytic run was performed in order to characterize the aldehyde produced by MBA partial oxidation. For this run 500 mL of 10 mM MBA solution and 0.6 g L<sup>-1</sup> of HP1/50 catalyst were used; the run lasted 12 h and a 75%

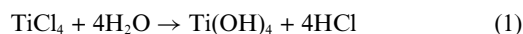
conversion of MBA was reached. In the course of this run no samples were withdrawn from the photoreactor. At the end of the run the whole suspension was filtered by using a paper filter (Whatman) and the catalyst was separated. Then the organic products present in the aqueous phase were extracted with CHCl<sub>3</sub> and concentrated by a rotovapor apparatus (model Buchi Rotovapor M). MBAD was separated by column chromatography by using a silica support (Silicagel 60, Merck) and a mixture of hexane and ethyl acetate (8 : 1 v/v) as the mobile phase. The recovered catalyst was used for performing another run at the same experimental conditions in order to check the occurrence of deactivation phenomena. The same results were obtained thus confirming, as expected, that in aqueous medium the TiO<sub>2</sub> catalyst shows a stable activity.

<sup>1</sup>H-, <sup>13</sup>C-NMR spectra were obtained by using a Bruker DPX FT NMR (500 MHz) spectrometer. The spectrometer was equipped with a 5 mm PABBO BB-inverse gradient probe. CDCl<sub>3</sub> was used as a solvent. Standard Bruker pulse programs (Bruker program 1D WIN-NMR, release 6.0) was used throughout the experiments.

### 3. Results and discussion

#### 3.1 Characterization of photocatalysts

Both the hydrolysis of TiCl<sub>4</sub> and subsequent condensation steps were carried out at room temperature, producing the photocatalysts with the following stoichiometric reactions:



The preparation conditions and some physical features of photocatalysts are summarized in Table 2. In agreement with the literature,<sup>8,9</sup> only nuclei of the thermodynamically stable rutile phase are formed in strongly acidic solution, even if at a very low precipitation rate. It has been found by us that only aging of the sol produces rutile crystals and that a decrease of the TiCl<sub>4</sub>/H<sub>2</sub>O v/v ratio lowers the time needed for crystal precipitation. For instance a catalyst was prepared with a TiCl<sub>4</sub>/H<sub>2</sub>O ratio of 0.1 for which the crystal precipitation started after only 50 days of aging. For this reason ratios higher than 0.05 (that of HP1/20) have not been used in the present investigation.

XRD patterns of HP and commercial samples are reported in Fig. 1. The peaks assignable to rutile are those at 2θ = 27.5°, 36.5°, 41°, 54.1° and 56.5°; it may be noted that the peaks of commercial rutile are well defined while those of all of the HP samples are broad, indicating that their crystallinity is low.

**Table 2** BET specific surface area (SSA), particle size and crystallite size of the photocatalysts

Catalyst	TiCl <sub>4</sub> /H <sub>2</sub> O v/v ratio	SSA/m <sup>2</sup> g <sup>-1</sup>	Aging time/days	Time for precipitation starting/days	Agglomerates size/nm	Crystallite size/nm
HP1/20	0.05	129	9	8	286	5.5
HP1/35	0.029	116	6	3	1050	5.6
HP1/50	0.02	118	6	3	719	6.8
HP1/75	0.013	125	4	2	304	7.1
HP1/100	0.01	135	4	2	244	6.1
SA	—	2.5	—	—	240	52

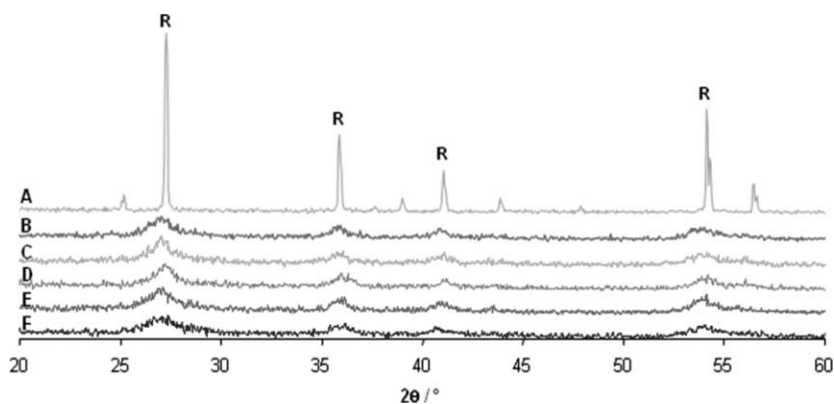


**Fig. 1** XRD patterns of HP and commercial TiO<sub>2</sub> samples; (A) SA, (B) HP1/100, (C) HP1/75, (D) HP1/50, (E) HP1/35, (F) HP1/20. “R” = rutile peaks.

Size values of primary crystallites (calculated using the Scherrer equation) were quite low (5.5–7.1 nm), and very similar to each other. The sizes of the crystallite aggregates were much higher (see Table 2), as estimated from SEM observations, and they increased with the increase of the TiCl<sub>4</sub>/H<sub>2</sub>O ratio, *i.e.* acidity, and the time needed for the starting of precipitation. The size values of agglomerates decreased from HP1/35 to HP1/100, but the situation for HP1/20 was quite different. Due to the high Ti/H<sub>2</sub>O ratio, the precipitation started only at the end of 8th day, so that the time allowed for particle aggregation (1 day) was much lower than that of all the other preparations. This fact should justify the low value of agglomerate size reported in Table 2 for HP1/20 sample.

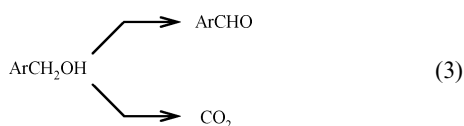
BET specific surface areas of HP samples are significantly higher than that of SA. The former ones, except that of HP1/20, increase with the decrease of agglomerate size.

### 3.2 Photoreactivity

In the initial part of this investigation, the photocatalytic oxidation of MBA was carried out by testing all the HP rutile catalysts together with the commercial one at equal reaction conditions.

No oxidation of MBA was observed in the absence of irradiation and/or catalyst and/or oxygen under the same experimental conditions used for the photoreactivity runs. Irradiation, catalyst and oxygen were all needed for the occurrence of the process.

All the photoreactivity runs indicated that the rates of formation of MBAD and CO<sub>2</sub> had values different from zero once the irradiation was turned on. These experiments confirmed that the MBA degradation<sup>17,19</sup> proceeds through two parallel pathways, both effective since the start of irradiation: (i) partial oxidation of MBA to the corresponding aldehyde, MBAD, which is released to the liquid phase and may compete with MBA for mineralization; and (ii) complete oxidation of MBA to CO<sub>2</sub> and H<sub>2</sub>O through intermediates which do not desorb from the catalyst surface. Eqn 3 describes the MBA degradation process:



Selectivity values depend on the competition between the two pathways; surface physico-chemical and structural properties of the photocatalysts are the most important factors influencing that competition, although other parameters like the structure of the starting aromatic molecule and its initial concentration cannot be neglected.

A run was carried out with a catalyst amount smaller than the optimal one in order to check if the absorbed photon flow affects the selectivity towards aldehyde. For this run performed by using 0.2 g L<sup>-1</sup> of the HP1/50 sample, Fig. 2 reports the MBA, MBAD and CO<sub>2</sub> concentration values and the carbon balance *versus* irradiation time. Overall conversion of MBA and selectivity to aldehyde are also reported (they are quoted to the right ordinate axis). The carbon balance has been performed by summing the MBA and MBAD concentrations to that of CO<sub>2</sub> concentration, by dividing by 8 the value obtained by TOC determination.

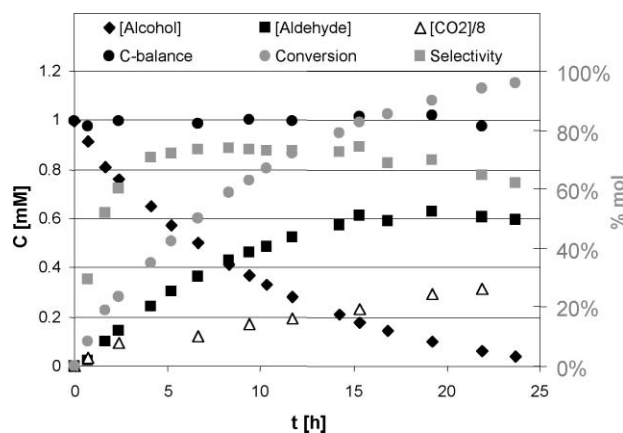


**Fig. 2** Experimental results of photocatalytic oxidation of MBA using the HP1/50 (0.2 g L<sup>-1</sup>) sample. Conversion and selectivity are scaled on the right side. The CO<sub>2</sub> concentration values were divided by 8 for normalization purposes.

It is worth noting that the slope of CO<sub>2</sub> concentration data is different from zero at zero time thus indicating that this CO<sub>2</sub> is not produced through subsequent oxidation of the initially produced MBAD released to the liquid phase. The selectivity values plateaued at their highest value in the conversion range of 20–80%. From 0 to 20% conversion, the selectivity increases

probably because of the occurrence of transient phenomena on the catalyst surface;<sup>22</sup> it must be underlined that the TOC and MBAD quantitative determinations at low MBA conversion may be strongly affected by experimental errors. For conversions higher than 80% the selectivity decreases along with the MBAD concentration in the liquid phase (see Fig. 2). In this condition the produced aldehyde molecules favourably compete with remaining alcohol molecules for adsorption and (photo)oxidation onto the surface sites. On the basis of this finding the comparison of catalyst performances has been done by determining the selectivity and the time needed for achieving a MBA conversion of 50%.

The photoreactivity results obtained with the HP and commercial (SA) catalysts are summarized in Table 3. This Table reports the reaction time needed for 50% MBA conversion,  $t_{1/2}$ , the corresponding selectivity to MBAD and the carbon balance percentage. It can be noticed that all the HP catalysts results are much more selective (*ca.* 2–4 fold) than SA, but the HP1/50 sample showed the highest selectivity (74%) towards MBAD production. To the best of our knowledge this value is the highest one ever reported in the literature for heterogeneous photocatalytic oxidation of alcohol to aldehyde in water. The HP1/35, HP1/75 and HP1/100 samples showed a similar selectivity, *i.e.* *ca.* 60%, while the HP1/20 sample the lowest one, *i.e.* 45%. The commercial catalyst, SA, which exhibits a selectivity far lower than those of HP samples, however gives rise to a similar reactivity, *i.e.*  $t_{1/2}$ .

The carbon balance, verified by taking into account only the unreacted alcohol, the produced aldehyde and CO<sub>2</sub>, was quite satisfied by the HP samples with higher selectivity (HP1/35 and HP1/50). It may be noted from the data in Table 3 that the failure on carbon balance increases with the decrease of the sample selectivity, being the highest one for the commercial sample (*i.e.* the one with the lowest selectivity). In the course of the photocatalytic runs, in addition to the main products of MBA oxidation, *i.e.* aldehyde and CO<sub>2</sub> (see eqn 3), hydroxylated aromatics, benzoic acids and open-ring products were also found. The amounts of these last products depended on the used photocatalyst; for the most selective HP samples only traces of them were found while for the others HP and the commercial sample the amounts were higher. It is likely that these products arise from the subsequent oxidation of produced aldehyde, being this pathway more relevant for the less selective, and therefore more oxidizing, samples.

**Table 3** Photocatalysts performance for MBA photo-oxidation to MBAD for 50% conversion

Catalyst	Catalyst amount/g L <sup>-1</sup>	$t_{1/2}$ /h	Selectivity (% mol)	C balance (%) <sup>a</sup>
HP1/20	0.2	2.3	45	91
HP1/35	0.6	3.6	60	96
HP1/50	0.2	6.65	74	99
HP1/50	0.6	2.6	72	98
HP1/75	0.2	2.95	55	94
HP1/100	0.2	3.3	61	96
SA	0.4	2.15	21	70

<sup>a</sup> C-balance was obtained as sum of MBA, MBAD and CO<sub>2</sub> concentration.

By comparing the results obtained from runs carried out with different amounts of HP1/50 (see Table 3), it may be noted that the use of lower amounts of photocatalyst (0.2 instead of 0.6 g L<sup>-1</sup>, three times less) gives rise to a small increase of the selectivity while the  $t_{1/2}$  increases about three times. By considering that the suspension with 0.2 g of catalyst absorbs about half of the photons absorbed with 0.6 g but that the photons absorbed per unit mass of catalyst increase about 150%, it can be concluded that the photoprocess is quite insensitive to the irradiation conditions, at least under the used experimental conditions.

In order to check the potentiality of this process as a green synthetic one, produced MBAD and residual MBA were separated, analysed and purified according to the procedure described in the experimental section. MBAD was isolated with a yield of *ca.* 48%. <sup>1</sup>H-NMR and <sup>13</sup>C-NMR analyses (see ESI†) confirmed that the obtained MBAD has a high purity (>99%).

In the last part of this study the effect of different substituent groups on the photoprocess performance was investigated with the aim of checking if the selectivity to the corresponding aldehyde is a feature of the photocatalyst or it is affected by the chemical nature of aromatic alcohol. The most selective sample, HP1/50, and the commercial one, SA, were used to carry out the photo-oxidation of benzyl alcohol (BA), 4-methylbenzyl alcohol (MeBA) and 4-nitrobenzyl alcohol (NBA). The photoreactivity results obtained with the 4-substituted alcohols are summarized in Table 4; the figures in Table 4 are the averages of three independent experiments.

A thorough investigation of the intermediates produced in the course of photocatalytic degradation was not the aim of this paper. As found with MBA, the oxidation of MeBA, BA, and NBA mainly produced the corresponding aldehydes and CO<sub>2</sub>, this finding suggesting that the mineralization of adsorbed alcohol molecules occurs by means of subsequent oxidative steps producing species which do not desorb from the photocatalyst surface to the solution. Small amounts of hydroxylated derivatives and open ring products were detected for NBA tested with HP1/50; their amounts were much higher when SA was used.

By taking as reference the unsubstituted benzyl alcohol, the data of Table 4 indicate that the presence of electron donor groups (–OCH<sub>3</sub> and –CH<sub>3</sub>) positively affects the selectivity for both photocatalysts, although the commercial sample (SA) shows in all cases the worst performance. On the contrary the electron withdrawing group (–NO<sub>2</sub>) was detrimental and a very scarce selectivity was observed. It can hence be stated that the presence of an electron withdrawing group such as –NO<sub>2</sub> favours the reaction pathway leading to the breakage of the aromatic ring with formation of over oxidised species and eventually CO<sub>2</sub>. The same behaviour was observed in the hydroxylation of various aromatic species.<sup>23a</sup> In that case it has been reported<sup>23</sup> that the presence of an electron donor group, due to its inductive and delocalization effects, hinders oxidant attacks towards the aromatic ring.

In reference to the oxidation rate, the data of Table 4 indicate that reaction times needed to achieve 50% conversion of alcohol decrease in the order: BA > MeBA > MBA while time was longer from BA to NBA. This order indicates that the reaction rate is enhanced by electron-donating substituents and retarded

**Table 4** Results of photocatalytic oxidation of BA, MBA, MeBA, NBA, using HP1/50 (0.6 g L<sup>-1</sup>) and SA samples (0.4 g L<sup>-1</sup>). The selectivity to aldehyde was determined for 50% conversion of alcohol

Catalyst	MBA		MeBA		BA		NBA	
	HP1/50	SA	HP1/50	SA	HP1/50	SA	HP1/50	SA
<i>t</i> <sub>1/2</sub> /h	2.6	2.15	4.2	4.2	6.5	3.8	9.8	6.7
Selectivity (% mol)	72	21	47	9.5	42	9.2	5.3	3.3
C Balance (% mol)	98	70	96	68	95	66	90	65
<i>k</i> <sub>0</sub> /h <sup>-1</sup>	0.267	0.266	0.165	0.265	0.107	0.182	0.07	0.073

by electron-withdrawing substituents. By considering that no correlation was found between reactivity and the water–octanol partition coefficients of aromatic alcohols (or aldehydes), it may be assumed that the electronic properties of substituent groups play a more significant role than the relative solubility in water of reagents and products. On this ground the influence of the substituent group on the rate of partial oxidation of aromatic alcohols can be interpreted in terms of Hammett's relationship.<sup>24</sup>

The basic Hammett equation is:

$$\log \left( \frac{k_{\text{PO}}}{k_{\text{PO}}^0} \right) = \rho \sigma \quad (4)$$

in which *k*<sub>PO</sub> is the kinetic constant of the partial oxidation reaction of the substituted reactant, *k*<sub>PO</sub><sup>0</sup> that of the unsubstituted reactant,  $\sigma$  the substituent constant which is related to the electron orientation effect of the specific substituent *R* and  $\rho$  the reaction constant which depends only on the type of reaction but not on the substituent used. The reaction constant, or sensitivity constant,  $\rho$ , describes the susceptibility of the reaction to substituents. A plot of ( $\log k_{\text{PO}}$ ) versus  $\sigma$  for a given reaction with many differently substituted reactants gives a straight line with slope equal to  $\rho$ .

In the present case the rates of overall oxidation of alcohol and of partial oxidation to aldehyde are well described by first order kinetics with respect to alcohol concentration:

$$-\frac{dC_{\text{ArOH}}}{dt} = k_0 C_{\text{ArOH}} = (k_{\text{min}} + k_{\text{PO}}) C_{\text{ArOH}} \quad (5)$$

$$\frac{dC_{\text{ArO}}}{dt} = k_{\text{PO}} C_{\text{ArOH}} \quad (6)$$

in which *C*<sub>ArOH</sub> and *C*<sub>ArO</sub> are the concentration of aromatic alcohol and aldehyde, respectively, *t* the irradiation time, *k*<sub>0</sub> the first order kinetic constant of overall oxidation reaction and *k*<sub>min</sub> that of mineralization reaction. Dividing eqn 6 for eqn 5 produces:

$$\frac{dC_{\text{ArO}}}{dC_{\text{ArOH}}} = \frac{k_{\text{PO}}}{k_{\text{min}} + k_{\text{PO}}} \quad (7)$$

Integration of eqn 7 with the condition that at the start of irradiation, *i.e.* for *C*<sub>ArOH</sub> = *C*<sub>ArOH,0</sub>, *C*<sub>ArO</sub> = 0 gives:

$$\frac{C_{\text{ArO}}}{C_{\text{ArOH},0} - C_{\text{ArOH}}} = \frac{k_{\text{PO}}}{k_{\text{min}} + k_{\text{PO}}} \quad (8)$$

The left hand side term of eqn 8 represents the reaction selectivity towards aldehyde, *S*, and the (*k*<sub>min</sub> + *k*<sub>PO</sub>) term is equal to *k*<sub>0</sub>. The values of *k*<sub>0</sub> may be determined by a best

fitting procedure applied to the experimental data of alcohol concentration versus time once integration of eqn 5 is performed. In this way the *k*<sub>PO</sub> values can be calculated as:

$$k_{\text{PO}} = S k_0 \quad (9)$$

Table 4 reports the values of *k*<sub>0</sub> obtained by a least-squares best fitting procedure applied to all the photoreactivity runs; the reported figure is the average of three independent experiments. By using eqn 9 the values of *k*<sub>PO</sub> have been calculated. Fig. 3 reports in a semilogarithmic plot the values of *k*<sub>PO</sub> versus the Hammett constant of each substituent group of the aromatic alcohol for both used catalysts. The solid straight lines through the data represent the Hammett relationship (eqn 4) best fitted to HP1/50 data (*R*<sup>2</sup> > 0.99) and SA ones (*R*<sup>2</sup> > 0.94). The  $\rho$  values obtained by the best fitting procedure are -3.32 and -2.75 for HP1/50 and SA, respectively. The very good proportional relationship shown in Fig. 3 confirms the influence of the electrophilic nature of the substituent on the photocatalytic partial oxidation of aromatic alcohols to aldehydes.

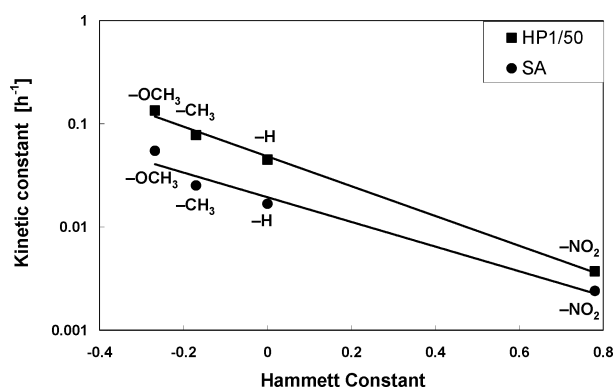


**Fig. 3** Correlation between the kinetic constant of partial oxidation reaction, *k*<sub>PO</sub>, and the Hammett constant.

## Conclusions

In conclusion the reported results indicate that heterogeneous photocatalytic methods may be used for synthesis of valuable organic compounds with selectivities as high as 74%. The rate of the process is that typical of heterogeneous photocatalytic systems but it could be enhanced by increasing the photon flow absorbed by the suspension, *i.e.* by using lamps of higher power; in this way also the process efficiency should improve. The catalyst preparation method and the photoprocess conditions obey the principles of green chemistry as neither organic solvents nor heavy-metal catalysts have been used. The whole process does not use or generate hazardous substances but it minimizes the

associated environmental impacts; moreover it would be able to reduce the amount of energy used in the process if photocatalysts that are able to use cheap and clean solar energy are developed. The investigation of the effect of the aromatic alcohol substituent on the partial oxidation performance shows that this effect is well described by the Hammett's relationship, whose validity is widely confirmed for homogeneous reacting systems but for very few cases<sup>25</sup> in heterogeneous photocatalytic systems.

## Acknowledgements

AA wish to thank Dr Güner Saka (Anadolu Üniversitesi-BİBAM Research Center, Eskişehir, Turkey) for NMR analyses.

## References

- 1 M. Schiavello, *Heterogeneous Photocatalysis*, John Wiley & Sons, New York, 1995.
- 2 S. Yang, Y. Liu, Y. Guo, J. Zhao, H. Xu and Z. Wang, *Mater. Chem. Phys.*, 2002, **77**, 501.
- 3 H. Kawaguchi and T. Wejima, *Kagaku Kogaku Ronbunshu*, 1983, **9**, 107.
- 4 H. Kawaguchi, *Environ. Technol. Lett.*, 1984, **5**, 471.
- 5 V. Augugliaro, L. Palmisano, A. Sclafani, C. Minero and E. Pelizzetti, *Toxicol. Environ. Chem.*, 1988, **16**, 89.
- 6 A. Sclafani, L. Palmisano and M. Schiavello, *J. Phys. Chem.*, 1990, **94**, 829, and references therein.
- 7 (a) M. Nag, P. Basak and S. V. Manorama, *Mater. Res. Bull.*, 2007, **42**, 1691; (b) S. Yin, R. Li, Q. He and T. Sato, *Mater. Chem. Phys.*, 2002, **75**, 76; (c) L. Li, J. Liu and Z. Jia, *Mater. Lett.*, 2006, **60**, 1753.
- 8 S. Yin, R. Li, Q. He and T. Sato, *Mater. Chem. Phys.*, 2002, **75**, 7.
- 9 S. Yang, Y. Liu, Y. Guo, J. Zhao, H. Xu and Z. Wang, *Mater. Chem. Phys.*, 2002, **77**, 501.
- 10 B. Fei, Z. Deng, J. H. Xin, Y. Zhang and G. Pang, *Nanotechnology*, 2006, **17**, 1927.
- 11 (a) Y. Mao and A. Bakac, *Inorg. Chem.*, 1996, **35**, 3925; (b) U. R. Pillai and E. S. Demessie, *J. Catal.*, 2002, **211**, 434.
- 12 M. A. Fox, H. Ogawa and P. Pichat, *J. Org. Chem.*, 1989, **54**, 3847.
- 13 A. Molinari, M. Bruni and A. Maldotti, *J. Adv. Oxid. Technol.*, 2008, **11**, 143.
- 14 A. Maldotti, A. Molinari and F. Bigi, *J. Catal.*, 2008, **253**, 312.
- 15 O. S. Mohamed, A. E. M. Gaber and A. A. Abdel-Wahab, *J. Photochem. Photobiol., A*, 2002, **148**, 205.
- 16 U. R. Pillai and E. Sahle-Demessie, *J. Catal.*, 2002, **211**, 434.
- 17 G. Palmisano, S. Yurdakal, V. Augugliaro, V. Loddo and L. Palmisano, *Adv. Synth. Catal.*, 2007, **349**, 964.
- 18 M. Addamo, V. Augugliaro, M. Bellardita, A. Di Paola, V. Loddo, G. Palmisano, L. Palmisano and S. Yurdakal, *Catal. Lett.*, 2008, **126**, 58.
- 19 S. Yurdakal, G. Palmisano, V. Loddo, V. Augugliaro and L. Palmisano, *J. Am. Chem. Soc.*, 2008, **130**, 1568.
- 20 V. Augugliaro, H. Kisch, V. Loddo, M. J. López-Muñoz, C. Márquez-Álvarez, G. Palmisano, L. Palmisano, F. Parrino and S. Yurdakal, *Appl. Catal., A*, 2008, **349**, 182.
- 21 V. Augugliaro, H. Kisch, V. Loddo, M. J. López-Muñoz, C. Márquez-Álvarez, G. Palmisano, L. Palmisano, F. Parrino and S. Yurdakal, *Appl. Catal., A*, 2008, **349**, 189.
- 22 S. Yurdakal, V. Loddo, G. Palmisano, V. Augugliaro and L. Palmisano, *Catal. Today*, 2008, DOI: 10.1016/j.cattod.2008.06.032.
- 23 (a) G. Palmisano, M. Addamo, V. Augugliaro, T. Caronna, E. García-López, V. Loddo and L. Palmisano, *Chem. Commun.*, 2006, **9**, 1012; (b) V. Augugliaro, T. Caronna, V. Loddo, G. Marci, G. Palmisano, L. Palmisano and S. Yurdakal, *Chem.–Eur. J.*, 2008, **14**, 4640; (c) E. Baciocchi, M. Bietti, B. Chiavarino, M. E. Crestoni and S. Fornarini, *Chem.–Eur. J.*, 2002, **8**, 532.
- 24 L. P. Hammett, *J. Am. Chem. Soc.*, 1937, **59**, 96.
- 25 (a) B. Sangchakr, T. Hisanaga and K. Tanaka, *J. Photochem. Photobiol., A*, 1995, **85**, 187; (b) K. Tanaka and K. S. N. Reddy, *Appl. Catal., B*, 2002, **39**, 305.